LOCALIZING VECTOR FIELD TOPOLOGY

Gerik Scheuermann, Bernd Hamann, and Kenneth I. Joy
Center of Image Processing and Integrated Computing, Department of Computer Science,
University of California, Davis, CA 95616-8562, U.S.A.
scheuer@ucdavis.edu, { hamann,joy } @cs.ucdavis.edu

Wolfgang Kollmann
Department of Mechanical and Aeronautical Engineering
University of California, Davis, CA 95616, U.S.A.
wkollmann@ucdavis.edu

Keywords: vector field, flow, topology, visualization

Abstract The topology of vector fields offers a well known way to show a "condensed" view of the stream line behavior of a vector field. The global structure of a field can be shown without time-consuming user interaction. With regard to large data visualization, one encounters a major drawback: the necessity to analyze a whole data set, even when interested in only a small region. We show that one can localize the topology concept by including the boundary in the topology analysis. The idea is demonstrated for a turbulent swirling jet simulation example. Our concept works for all planar, piecewise analytic vector fields on bounded domains.

Introduction

Vector fields are a major "data type" in scientific visualization. In fluid mechanics, velocity and vorticity are given as vector fields. This holds also for pressure or density gradient fields. Electromagnetics is another large application area with vector fields describing electric and magnetic forces. In solid mechanics, displacements are typical vector fields under consideration. Science and engineering study vector fields in different contexts. Measurements and simulations result in large data sets with vector data that must be visualized. Besides interactive and texture-based methods, topological methods have been studied by the visualization community, see Helman and Hesselink, 1990, Globus et al., 1991 for example. In most cases, the scientist or engineer is in-

terested in integral curves instead of the vector field itself. Since the behavior of curves differs, a natural approach is to study classes of equivalent curves. This approach reduces the information concerning all curves to the information about the structural changes of curves. Vector field topology is one answer to this question. First, one detects all stationary curves, i. e., the critical points (or zeros) in the vector field. Then, one finds all integral curves where the behavior is different between the neighboring curves. These "separatrices" are then visualized together with the critical points, providing a detailed description of the behavior of the integral curves.

A major drawback of topology-based visualization is the fact that one must analyze the whole data set. In many situations, a scientist or engineer would like to understand the behavior of curves in a limited area only. Due to the global nature of topology, one analyzes, up to now, the whole data set to find all separatrices in this area. In this paper, we show that this is not necessary. By a strict topological analysis of the boundary (of the local region of interest), we find all structural changes of the integral curves in any bounded region without touching data outside the region. We start by providing a rigorous mathematical treatment of these concepts. We continue with algorithmic details and conclude with theoretical and practical examples.

1. VECTOR FIELD TOPOLOGY

Scientific visualization is concerned with bounded vector fields, in most cases. In this paper, we deal only with two-dimensional vector fields, and we provide the definitions only for this case.

Definition 1.1 *A* **planar vector field** *is a map*

$$\begin{aligned} v : \mathrm{R}^2 \supset D &\rightarrow \mathrm{R}^2 , \\ x &\mapsto v(x) . \end{aligned} \tag{1.1}$$

D *is called* **domain** *of the vector field.*

The domain D is usually given as a grid consisting of cells with the vector data either given at the vertices, edges or cell centers. An interpolation method is used to create a continuous vector field description for the whole domain. For this reason, we assume that the vector field consists of a finite number of "analytic pieces" (one for each cell) that are glued together along the grid edges, thus defining a continuous vector field. As mentioned, a scientist or engineer is often more interested in the integral curves.

Definition 1.2 *An* **integral curve through a point** $x \in D$ *of a vector field* $v : \mathrm{R}^2 \supset D \rightarrow \mathrm{R}^2$ *is a map*

$$c_x : \mathrm{R} \supset I \rightarrow D , \tag{1.2}$$

where

$$c_x(0) = x_0\,, \tag{1.3}$$
$$\dot{c}_x(t) = v\left(c(t)\right)\,, \qquad \forall\, t \in I\,. \tag{1.4}$$

The theory of ordinary differential equations states that integral curves exist and are unique if the vector field is continuous and satisfies the Lipschitz condition. This is the case for all interpolation schemes used in visualization. Topology is especially of interest when concerned with the asymptotic behavior of integral curves. "Limit sets" is the term used for start and end of integral curves.

Definition 1.3 *Let $v : D \to \mathrm{R}^2$ be a Lipschitz-continuous vector field and $c : \mathrm{R} \to D$ an integral curve. The set*

$$\{a \in D | \exists (t_n)_{n=0}^{\infty} \subset \mathrm{R}, t_n \to \infty, \lim_{n\to\infty} c(t_n) \to a\} \tag{1.5}$$

is called ω**-limit set of** *c. The set*

$$\{a \in D | \exists (t_n)_{n=0}^{\infty} \subset \mathrm{R}, t_n \to -\infty, \lim_{n\to\infty} c(t_n) \to a\} \tag{1.6}$$

is called α**-limit set of** *c.*

Remark 1.4 *In the case of a curve c leaving the domain, we consider the last boundary point as its ω-limit set. In the case of a curve c starting at the boundary, we call its first point on the boundary its α-limit set.*

We limit the types of limit sets in this paper to critical points and the inflow and outflow parts of the boundary, since these are the most common cases.

Definition 1.5 *A* **critical point** *of $v : D \to \mathrm{R}^2$ is a point $p \in D$ with $v(p) = 0$. If all integral curves in a neighborhood of the critical point p have the point p as α-limit set, the point p is called a* **source***. If all integral curves in a neighborhood of the critical point p have the point p as ω-limit set, the point p is called a* **sink***. If a positive finite number of integral curves have the point p as α- or ω-limit set, we call the point p a* **saddle***.*

The boundary is split into inflow, boundary flow, and outflow regions.

Definition 1.6 *Let $D \subset \mathrm{R}^2$ be a compact domain of a Lipschitz-continuous vector field $v : D \to \mathrm{R}^2$. Let $d \in \partial D$ be a point on the boundary. We define the following three entities:*

(1) The point d is called an **outflow point** *if every integral curve through d ends at d and there exists an integral curve through d that does not*

contain another point of ∂D. The set of all outflow points is called **outflow set**.

(2) The point d is called an **inflow point** *if every integral curve through d starts at d and there exists an integral curve through d that does not contain another point of ∂D. The set of all inflow points is called* **inflow set**.

(3) The point d is called a **boundary flow point** *if there exists an integral curve $\alpha_d : (-\epsilon, \epsilon) \to D$, $\epsilon > 0$, through d lying completely inside ∂D. The set of all boundary flow points is called* **boundary flow set**.

A point $d \in \partial D$ that is not an inflow, outflow, or boundary flow point is called **boundary saddle**.

Each integral curve has an α limit set and an ω limit set. We can also construct the union of all integral curves that have a particular α or ω set. These basins are at the center of topology analysis, and visualization, as we will see.

Definition 1.7 *Let $v : D \to \mathrm{R}^2$ be a Lipschitz-continuous vector field and $A \subset D$ a subset. The union of all integral curves of v that converge to A for $t \to -\infty$ is called* **α-basin of** *A, denoted by $B_\alpha(A)$. Let $\Omega \subset D$ be a subset. The union of all integral curves of v that converge to Ω for $t \to \infty$ is called* **ω-basin of** *Ω, denoted by $B_\omega(\Omega)$.*

Since integral curves exist through every point, are unique, do not cross and have a single α- or ω-basin, we obtain a description of the domain D as a disjoint union of α-basins and as a disjoint union of ω-basins.

Theorem 1 *Let $D \subset \mathrm{R}^2$ be a compact subset. Let $v : D \to \mathrm{R}^2$ be a Lipschitz-continuous vector field. Let $a_1, \ldots, a_j$ be the sources, $s_1, \ldots, s_k$ be the saddles, $b_1, \ldots, b_p$ be the boundary saddles, and $z_1, \ldots, z_l$ be the sinks. Furthermore, let $I_1, \ldots, I_m$ be the inflow components, and $O_1, \ldots, O_n$ be the outflow components. If we assume that there are no other α- and ω-limit sets, then D can be decomposed into α-basins,*

$$D = \bigcup_{i=1}^{j} B_\alpha(a_i) \cup \bigcup_{i=1}^{m} B_\alpha(I_i) \cup \bigcup_{i=1}^{l} B_\alpha(s_i) \cup \bigcup_{i=1}^{p} B_\alpha(b_i) \cup \bigcup_{i=1}^{n} O_i \cup \bigcup_{i=1}^{k} \{z_i\}\,. \tag{1.7}$$

The region D can also be divided into ω-basins,

$$D = \bigcup_{i=1}^{k} B_\omega(z_i) \cup \bigcup_{i=1}^{n} B_\omega(O_i) \cup \bigcup_{i=1}^{l} B_\omega(s_i) \cup \bigcup_{i=1}^{p} B_\omega(b_i) \cup \bigcup_{i=1}^{m} I_i \cup \bigcup_{i=1}^{j} \{a_i\}\,. \tag{1.8}$$

The topology of a planar vector field is now defined as the union of all connected intersections of α-basins with ω-basins.

Definition 1.8 *Let $v : \mathrm{R}^2 \supset D \to \mathrm{R}^2$ be a Lipschitz-continuous vector field. Its* **topological information** *consists of two parts:*

(i) All α- and ω-limit sets including the connected inflow and outflow components of the boundary and the boundary saddles and

(ii) all connected components of the intersections of α-basins with ω-basins.

The idea of topology-based visualization is to extract this information from the data automatically and present it to the user for interactive data exploration.

2. TOPOLOGICAL ANALYSIS

We want to extract the topological information of a vector field given by a grid and vector values associated with vertices, edges or cells. After defining an interpolation scheme, we have a Lipschitz-continuous vector field in the sense of the previous section. The next step is to find the limit sets. Since we limit their types to critical points and parts of the boundary, we have to consider only these. Critical points are zeros of the vector field, so we must determine all zeros in each cell. Furthermore, we have to analyze their types to find sources, sinks, and saddles. This is necessary to find the basins in the second step. Our vector field is at least C^1-continuous inside the cells, so we can compute the derivative at critical points inside cells. This allows a simple classification in most cases.

Theorem 2 *Let $v : \mathrm{R}^2 \supset D \to \mathrm{R}^2$ be a vector field and p a critical point. If the derivative $Dv : D \to \mathrm{R}^2 \times \mathrm{R}^2$ is defined at p and has a determinant different from zero, the following classification of the critical point can be made:*

(a) If the real parts of both eigenvalues of $Dv(p)$ are positive, p is a source.

(b) If the real parts of both eigenvalues of $Dv(p)$ are negative, p is a sink.

(c) If the real parts of the two eigenvalues of $Dv(p)$ are of different signs, p is a saddle point. There are four integral curves reaching the saddle in the directions associated with the two eigenvalues.

If the assumptions in the previous theorem are not satisfied, one has to analyze the behavior of the integral curves in the neighborhood of the critical points. For an arbitrary interpolation scheme, this may be a difficult and expensive operation. For linear interpolations, a description is given in Tricoche et al., 2000. Since the analysis of critical points has been described before, we do not discuss details here. The second part is the analysis of the boundary. A general boundary consists of several smooth edges (often line segments), continuously

connected at vertices defining one or more closed curves. We consider first the case with a unique normal at the boundary point. This is valid inside the edges and in case of G^1-continuous connections of the edges.

Lemma 2.1 *Let $D \subset \mathrm{R}^2$ be a compact domain with a boundary ∂D consisting of a finite number of smooth curves (edges) so that no more than two edges have a point in common. Let $v : D \to \mathrm{R}^2$ be a Lipschitz-continuous, piecewise smooth vector field. Let $p \in \partial D$ be a point on the boundary with $v(p) \neq 0$ such that there is a unique outward directed normal $n(p) \in \mathrm{R}^2$ of the boundary at p. Then we have to consider four cases:*

(1) If $v(p) \cdot n(p) > 0$ holds, p is an outflow point.

(2) If $v(p) \cdot n(p) < 0$ holds, p is an inflow point.

(3) If $v(p) \cdot n(p) = 0$ holds and we have outflow (inflow, boundary flow) on both sides of p, p is an outflow (inflow, boundary flow) point.

(4) If $v(p) \cdot n(p) = 0$ holds and we have different behavior on the two sides of p, p is a boundary saddle. If we have inflow on the side pointed to by $v(p)$, we have to calculate a separatrix in this direction. If we have outflow on the side pointed to by $-v(p)$, we have to calculate a separatrix in this direction.

Lemma 2.1 is illustrated in Figure 1. In an implementation, this is quite abstract, since the last two expressions cannot be tested directly and it might seem difficult to test all points on one edge. The strategy is to find all zeros of the term $v(d) \cdot n(d)$ and check the behavior between the closest such points and p. For all common interpolation schemes, one can use standard numerical zero search and analysis methods for this problem. The analysis of boundary vertices is somewhat more involved, since one has to look at the geometry of the boundary at the vertex. We discuss the cases of a convex and a concave vertex separately in the next two lemmata.

Lemma 2.2 *Let $D \subset \mathrm{R}^2$ be a compact domain with a boundary ∂D consisting of a finite number of smooth curves (edges) so that no more than two edges have a point in common. Let $v : D \to \mathrm{R}^2$ be a Lipschitz-continuous, piecewise smooth vector field. Let $p \in \partial D$ be a point on the boundary between two smooth edges. There are two normals $m, n \in \mathrm{R}^2$ at p with respect to the edges. We assume that p is a convex corner, i. e. there is a convex neighborhood of p in D. Then we have to consider five cases:*

(A1) If $(v(p) \cdot m)\,(v(p) \cdot n) < 0$ holds, the integral curve through p in D contains only p.

(A2) If $(v(p) \cdot m)\,(v(p) \cdot n) > 0$ holds, p is an outflow or inflow point, depending on the common sign of the products.

(A3) If $v(p) \cdot m = 0$ and $v(o) \cdot m > 0$ holds for points $o \in \partial D$ arbitrary close to p on the first neighboring edge, p is a outflow point.

(A4) If $v(p) \cdot m = 0$ and $v(o) \cdot m = 0$ holds for points $o \in \partial D$ arbitrary close to p on the first neighboring edge, p is a boundary saddle. (The integral curve through p stays on the first edge and leaves D at p, so one does not have a separatrix entering the interior of D at p.)

(A5) If $v(p) \cdot m = 0$ and $(v(o) \cdot m) < 0$ holds for points arbitrary close to p on the first neighboring edge, p is a boundary saddle. (The integral curve through p consists only of p, so one has no separatrix entering the interior of D at p.)

An analysis of the cases with $v(p) \cdot n = 0$ yields the same results.

Lemma 2.2 is illustrated in Figure 2. The last case deals with a concave vertex.

Lemma 2.3 *Let $D \subset \mathrm{R}^2$ be a compact domain with a boundary ∂D consisting of a finite number of smooth curves (edges) so that no more than two edges have a point in common. Let $v : D \to \mathrm{R}^2$ be a Lipschitz-continuous, piecewise smooth vector field. Let $p \in \partial D$ be a point on the boundary between two smooth edges. There are two normals $m, n \in \mathrm{R}^2$ at p with respect to the edges. We assume that p is a concave corner, i. e. there is a convex neighborhood of $bar\mathrm{R}^2 - D$. Then we have to consider five cases:*

(C1) If $((v(p) \cdot m) (v(p) \cdot n)) > 0$ holds, p is either an outflow or an inflow point, depending on the common sign of the products.

(C2) If $((v(p) \cdot m) (v(p) \cdot n)) < 0$ holds, p is a boundary saddle. (The integral curve through p is a separatrix that has to be integrated backward and forward in time.)

(C3) If $v(p) \cdot m = 0$ and $v(o) \cdot m > 0$ holds for points $o \in \partial D$ arbitrary close to p on the first neighboring edge, the integral curve through p is a separatrix that has to be integrated backward and forward in time.

(C4) If $v(p) \cdot m = 0$ and $v(o) \cdot m < 0$ holds for points $o \in \partial D$ arbitrary close to p on the first neighboring edge, p is an inflow point.

(C5) If $v(p) \cdot m = 0$ and $v(o) \cdot m = 0$ holds for points $o \in \partial D$ arbitrary close to p on the first neighboring edge, the integral curve through p stays on one edge and enters the interior of D at p, so one has to calculate one part of the curve.

An analysis of the cases where $v(p) \cdot n = 0$ holds, yields the same results. The situation of the previous lemma is illustrated in Figure 3. As before, the algorithm determines all zeros of $v(d) \cdot m(d)$ and $v(d) \cdot n(d)$ on the two edges, and

analyzes the behavior of the points between the zeros closest to p. These lemmata allow to extract the first part of the topology information. The description of the basins uses an important fact: The α basins belonging to sources and inflow components are open two-dimensional subsets of D. The ω basins belonging to sinks and outflow components are also open two-dimensional subsets of D. Therefore, the boundaries of their intersections must either belong to one-dimensional basins or be curves through boundary saddles. The only limit sets with one-dimensional basins, under our assumptions, are saddles. Therefore, all intersections can be shown by drawing all one-dimensional basins of saddles, i. e., the integral curves starting or ending there and the integral curves through boundary saddles. This provides the second part of the topological information.

We focus on the fact that one can do this analysis on any bounded region of our data set and obtain useful information. The next two sections show applications and compare local and global topology. Up to now, visualization has not considered much boundary analysis since, in many applications, the boundary has a rather simple flow structure. Parts are set to zero, defined as outflow or inflow, so that there are no or only a few basin borders missing in global topology. This changes when "taking out" a region from a rather complex vector field.

3. ANALYTIC EXAMPLES

The considerations from the last section aim at an analysis of vector field topology including the boundary. The example provided in this section shows the effect of this analysis on the understanding of topological vector field structure. It is based on the study of vector fields given by polynomial equations. The construction of these fields is based on considerations based on *Clifford algebra*, see Scheuermann et al., 1998 and Scheuermann, 1999. Figures 4-6 show unit vectors to indicate the orientation of separatrices and integral curves. Critical points are red, green, or blue. Red color indicates a saddle point, green color a source, and blue color a sink. The separatrices are drawn in blue, integral curves are violet, and the boundaries of regions and domains are white.

We start with a vector field containing two sinks and two sources in a rectangular area. The conventional analysis, based on the separatrices starting at saddle points alone, will find no separating curves at all, so a scientist is left with the question of how the two sources and sinks interact. This can be seen in Figure 4. Since there exist integral curves from one source to both sinks, and also to the boundary, not all integral curves belong to the same open basin. We know that, as a result of the piecewise linear interpolation and the analytic structure of the original field, there are no additional critical points or more complicated structures involved (in this example). There are ten boundary sad-

dles where the flow turns from inflow to outflow. By starting the construction of separatrices at these positions it is possible to determine the structure of the flow. The result is shown in Figure 5. The whole rectangle is now divided into open basins with the same α- and ω-basin. Every integral curve in one of these basins starts and ends at the same critical point or connected component of the boundary. It is now easy to understand the interactions of the sinks and sources.

As mentioned before, this example was constructed using an analytic field description. The structure of the entire field is shown in Figure 6. The small white box marks the domain of our example. There are three saddle points where 12 separatrices start. The importance of the saddles for the standard analysis is seen by comparing the result inside the rectangle with the result shown in Figure 4.

4. APPLICATION EXAMPLE

We have applied the local topology extraction to a vortex breakdown simulation. Vortex breakdown is a phenomenon observed in a variety of flows ranging from tornadoes to wing tip vortices (Lambourne and Bryer, 1961), pipe flows (Sarpkaya, 1971, Faler and Leibovich, 1977, Leibovich, 1984, Lopez, 1990, Lopez, 1994) and swirling jets (Billant et al., 1999). The latter flows are important to combustion applications where they create recirculation zones with sufficient residence time for the reactions to approach completion. The example vector field contains 39909 data points and 79000 triangles. The piecewise linear interpolation contains 703 simple critical points, creating a complex global topology. First, we used a rectangle, shown in Figure 7. The data in this rectangle was used to analyze the local topology. We extracted all critical points and determined all boundary saddles by analyzing the boundary of the rectangle. This resulted in the topological structure shown in Figure 8. One can see some of the additional separatrices starting at the boundary saddles; they separate regions of flow staying inside the boundary from outflow and inflow parts. No analysis of data outside the rectangle was used. The required computing time does only depend on the size of the region and is (nearly) independent of the size of the overall data set.

It is possible to consider multiple regions of interest in the same data set to be analyzed independently. One may also use arbitrary polygons as boundaries. This is demonstrated in our second analysis of the same jet data set for which we chose three regions, shown in Figure 9. One region covers a part of the backstream besides the main inflow jet. The second region shows a part of the rectangle we used before. Neither of these two regions contains critical points, which makes boundary analysis necessary. The third region shows the mixing of the jet and the fluid downstream. Figure 10 shows the first two re-

gions in more detail. One can see clearly forward- and backward-facing flow. Without an analysis of the boundary, one obtains no separatrices due to the lack of critical points inside the two regions. The third region is shown in more detail in Figure 11. Since the analysis is limited to a rather small area, it can be analyzed quickly. One can depict several separatrices spiraling around critical points. The critical points inside these areas have Jacobians with complex conjugate eigenvalues, thus they are spirals; the real parts of the eigenvalues may have small absolute values, and a stream line in the neighborhood of the critical points approaches them very slowly.

5. CONCLUSIONS

We have presented a method to analyze the local topology of arbitrary regions in 2D vector fields. Our method is based on the idea of extracting the critical points in the domain and examining the region's boundary. By determining the inflow, outflow, and boundary flow segments one can separate the domain into regions of topologically uniform flow. We have discussed the differences to a global topology analysis approach in theory and applications, demonstrating the relevance of our localized approach when applied to regions with complicated flow patterns on the boundary. This case is typical of most interesting regions inside a larger data set.

Another important situation that we have studied is the absence of critical points in a region that provides interesting structure, like backward-facing flow. Our algorithm detects these areas and separates them from other parts of the flow leading to better visualizations of the local flow structure. Since the local topology analysis does not use any information outside a region of interest, it is very attractive when analyzing large data sets locally due to the significant reduction in computing time. Nevertheless, it must be mentioned that the separatrices in the local topology may differ from global topology, since they depend solely on the inflow/outflow switches on the boundary. For further research, the inclusion of limit cycles in the local topology is an important issue.

Acknowledgments

This work was supported by the National Science Foundation under contracts ACI 9624034 (CAREER Award), through the Large Scientific and Software Data Set Visualization (LSSDSV) program under contract ACI 9982251, and through the National Partnership for Advanced Computational Infrastructure (NPACI); the Office of Naval Research under contract N00014-97-1-0222; the Army Research Office under contract ARO 36598-MA-RIP; the NASA Ames Research Center through an NRA award under contract NAG2-1216; the Lawrence Livermore National Laboratory under ASCI ASAP Level-2 Memorandum Agreement B347878 and under Memorandum Agreement B503159; the Lawrence Berkeley National Laboratory; the Los

Alamos National Laboratory; and the North Atlantic Treaty Organization (NATO) under contract CRG.971628. We also acknowledge the support of ALSTOM Schilling Robotics and SGI. We thank the members of the Visualization and Graphics Research Group at the Center for Image Processing and Integrated Computing (CIPIC) at the University of California, Davis.

References

Billant, P., Chomaz, J., and Huerre, P. (1999). Experimental Study of Vortex Breakdown in Swirling Jets. *Journal of Fluid Mechanics*, 376:183 – 219.

Faler, J. H. and Leibovich, S. (1977). Disrupted States of Vortex Flow and Vortex Breakdown. *Physics of Fluids*, 96:1385 – 1400.

Globus, A., Levit, C., and Lasinski, T. (1991). A Tool for Visualizing the Topology of Three-Dimensional Vector Fields. In Nielson, G. M., Rosenblum, L. J., editors, *IEEE Visualization '91*, IEEE Computer Society Press, Los Alamitos, CA, pages 33 – 40..

Helman, J. L. and Hesselink, L. (1990). Surface Representations of Two- and Three-Dimensional Fluid Flow Topology. In Nielson, G. M. and Shriver, B., editors, *Visualization in scientific computing*, IEEE Computer Society Press, Los Alamitos, CA, pages 6–13.

Lambourne, N. C. and Bryer, D. W. (1961). The Bursting of Leading Edge Vortices: Some Observations and Discussion of the Phenomenon. *Aeronautical Research Council R. & M.*, 3282:1 – 36.

Leibovich, S. (1984). Vortex Stability and Breakdown: Survey and Extension. *AIAA Journal*, 22:1192 – 1206.

Lopez, J. M. (1990). Axisymmetric Vortex Breakdown. part 1. confined Swirling Flow. *Journal of Fluid Mechanics*, 221:533 – 552.

Lopez, J. M. (1994). On the Bifurcation Structure of Axisymmetric Vortex Breakdown in a Constricted Pipe. *Physics of Fluids*, 6:3683 – 3693.

Sarpkaya, T. (1971). On Stationary and Travelling Vortex Breakdown. *Journal of Fluid Mechanics*, 45:545 – 559.

Scheuermann, G. (1999). *Topological Vector Field Visualization with Clifford Algebra*. dissertation, Computer Science Department, University of Kaiserslautern, Kaiserslautern, Germany.

Scheuermann, G., Hagen, H., and Krüger, H. (1998). An Interesting Class of Polynomial Vector Fields. In Dæhlen, M., Lyche, T., and Schumaker, L. L., editors, *Mathematical Methods for Curves and Surfaces II*, pages 429–436, Nashville.

Tricoche, X., Scheuermann, G., and Hagen, H. (2000). A topology simplification method for 2d vector fields. In Ertl., T., Hamann, B. and Varshney,

A., editors, *IEEE Visualization 2000*, IEEE Computer Society Press, Los Alamitos, CA, pages 359 – 366.

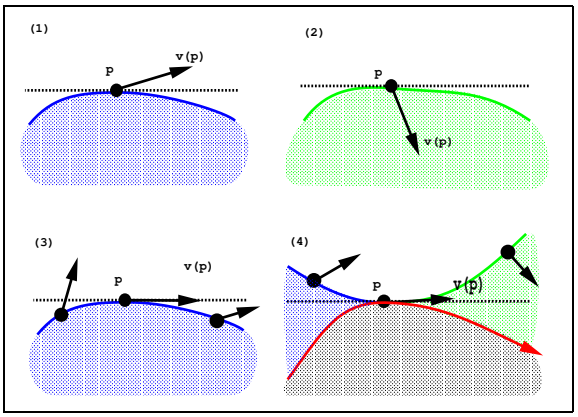

Figure 1 Regular vertex. Case (1): outflow point; case (2): inflow point; case (3): flow parallel to the boundary tangent — outflow on both sides of p; case (4) : flow parallel to the boundary tangent — outflow on the $-v(p)$ side and inflow on the other side.

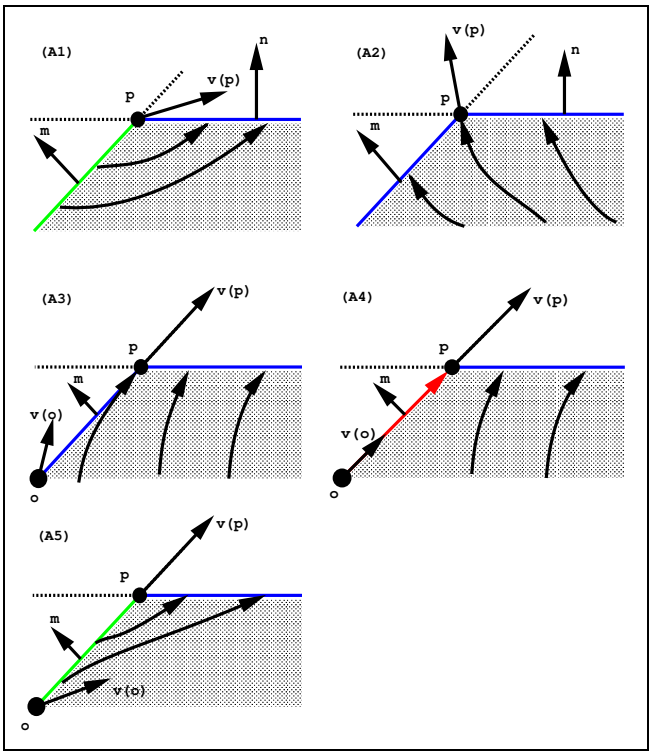

Figure 2 Convex vertex. Case (A1): inflow and outflow around p; case (A2): outflow on both sides of p; case (A3): flow at vertex being parallel to one tangent — outflow around p; case (A4): boundary flow on one side — outflow on the other side; case (A5): flow at vertex parallel to one tangent, inflow on one side, and outflow on the other side. Inflow is marked green, outflow is marked blue, and boundary flow is marked red.

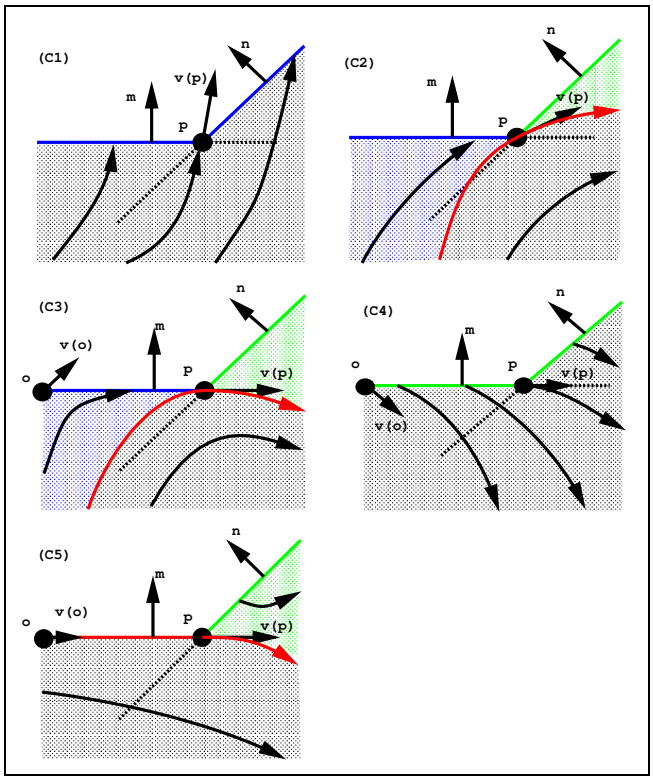

Figure 3 Concave vertex. Case (C1): outflow on both sides of p; case (C2): outflow on one side and inflow on the other side; case (C3): flow parallel to one tangent at vertex p, outflow on one side, and inflow on the other side; case (C4): flow parallel to one tangent at vertex p and inflow on both sides; case (C5): boundary flow on one side and inflow on the other side. Inflow and α-basins are colored green, outflow and ω-basins are colored blue, and separatrices and boundary flow are shown in red color.

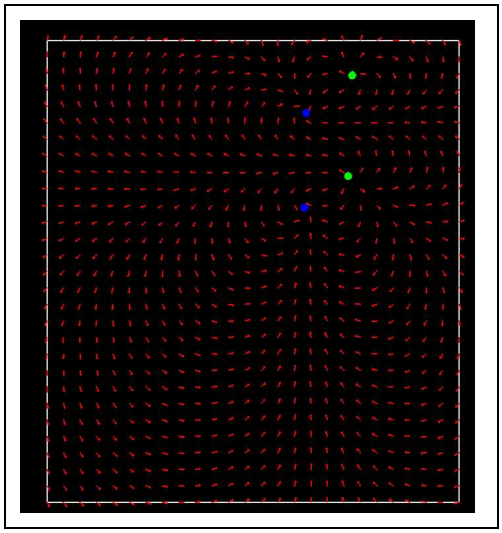

Figure 4 Vector field containing two sources and two sinks.

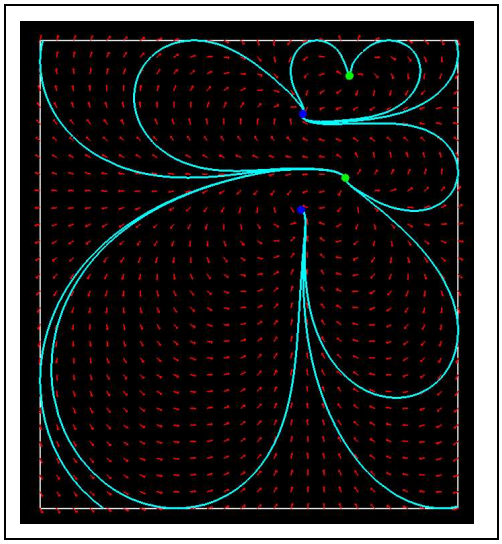

Figure 5 Local topology showing interaction of sources and sinks.

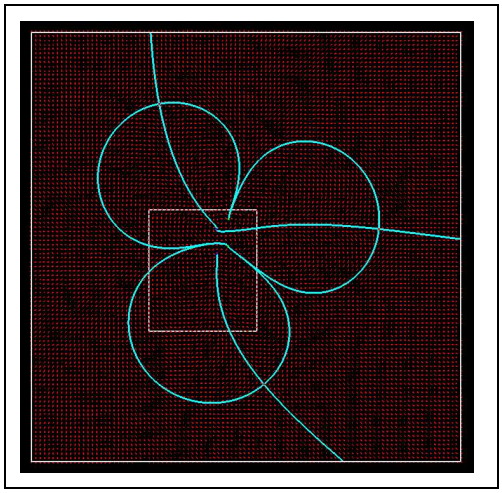

Figure 6 Global topology derived by considering entire field.

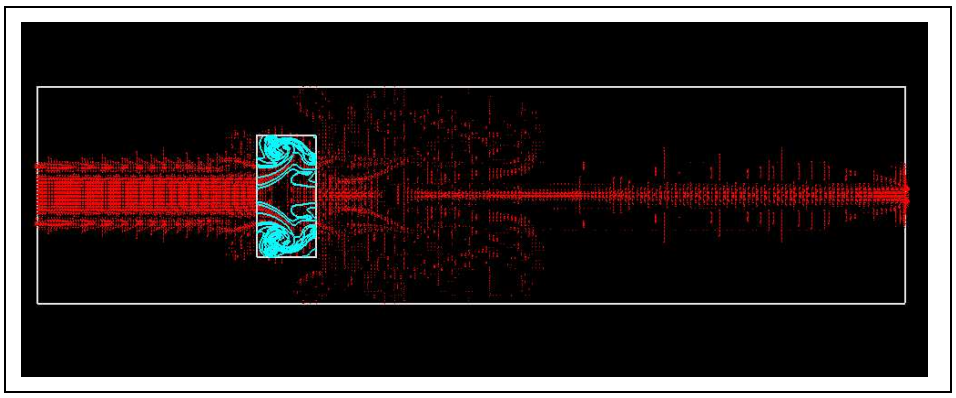

Figure 7 Rectangular region in jet data set and result of local topology analysis.

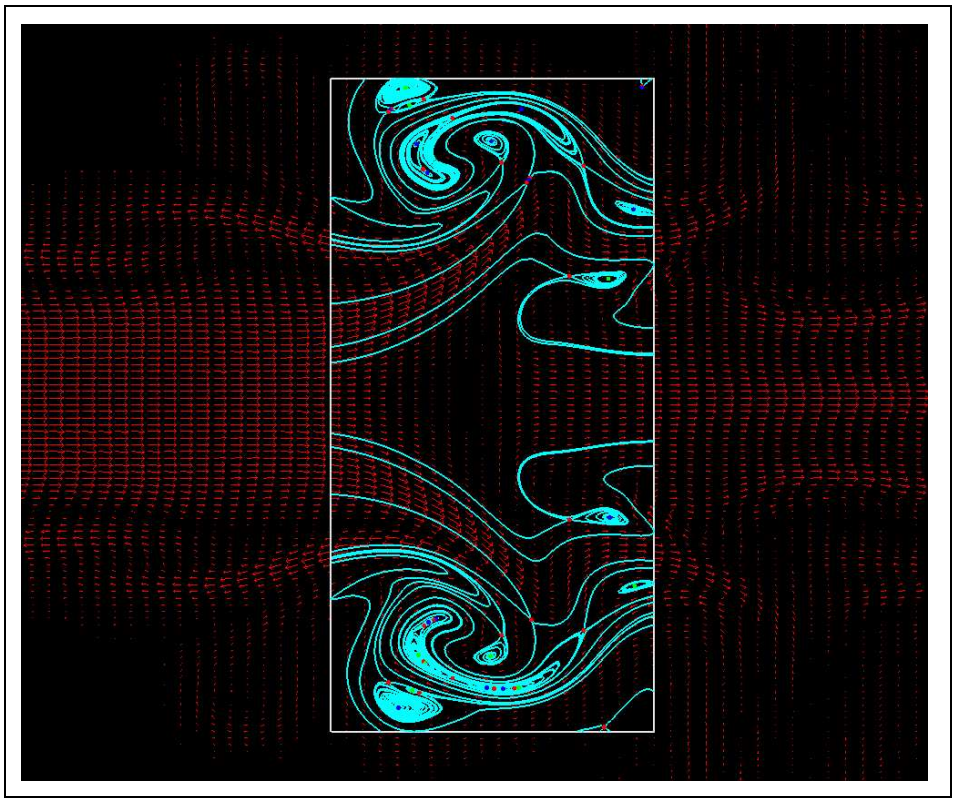

Figure 8 Magnification of result of local topology analysis shown in Figure 7.

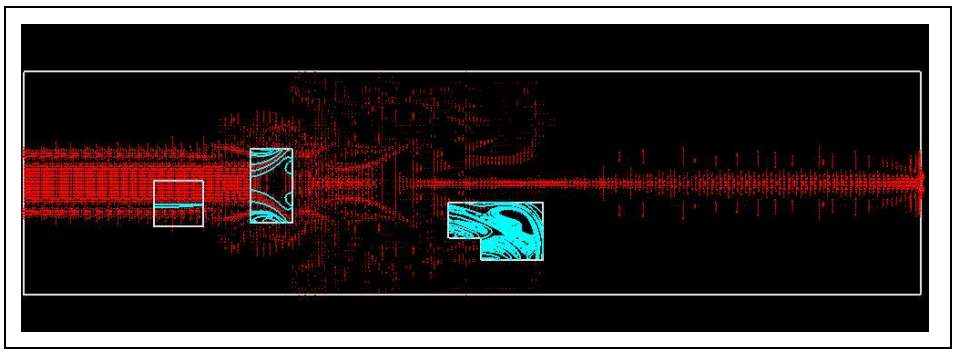

Figure 9 Three regions in jet data set and respective results of local topology analysis.

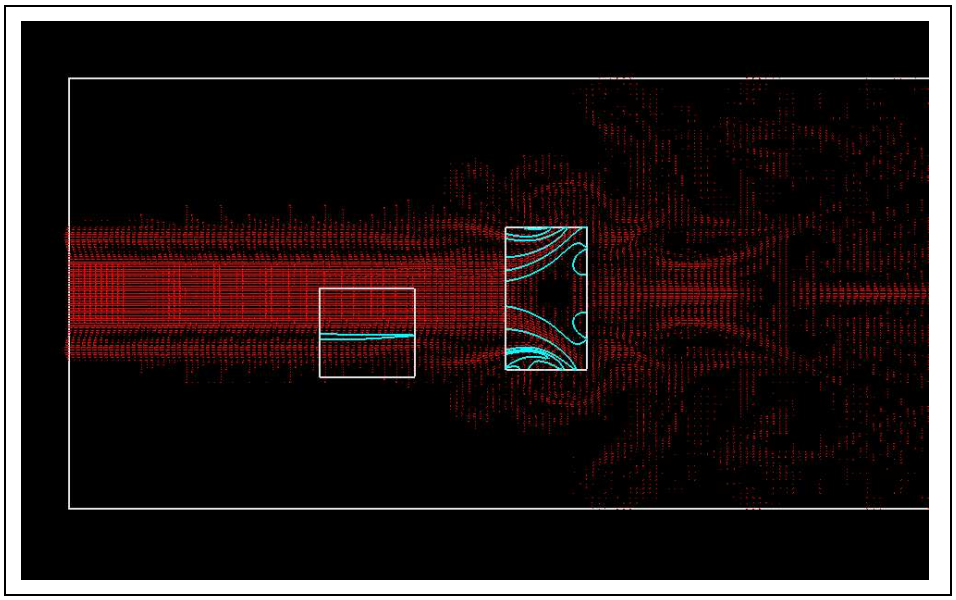

Figure 10 Local topology analysis inside two regions without critical point (jet data set).

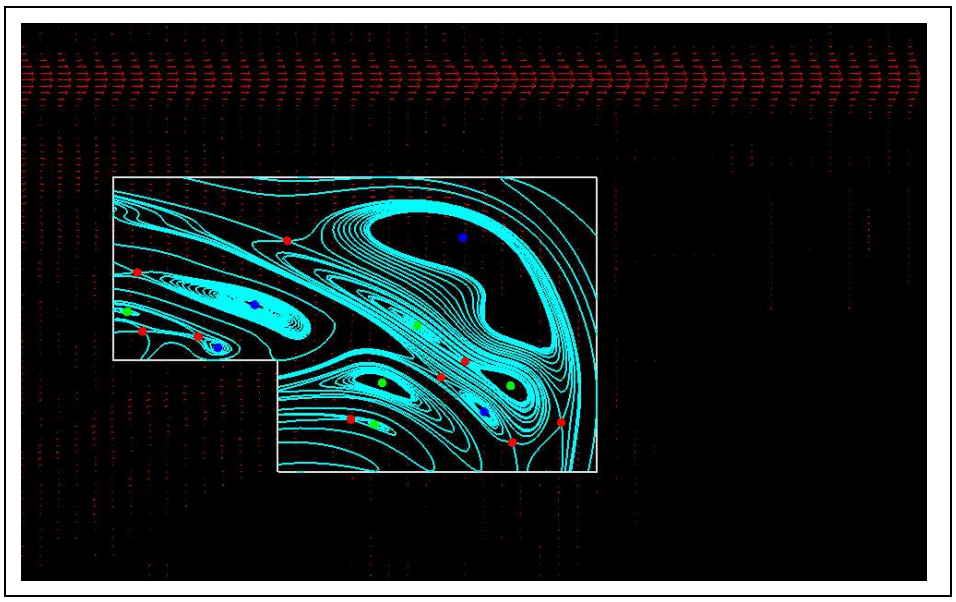

Figure 11 Local topology analysis result of highly complicated region (jet data set).